Biosensors and Bioelectronics 131 (2019) 178–184

Contents lists available at ScienceDirect

Biosensors and Bioelectronics

journal homepage: www.elsevier.com/locate/bios

Engineering of $CdTe/SiO_2$ nanocomposites: Enhanced signal amplification and biocompatibility for electrochemiluminescent immunoassay of alpha-fetoprotein

Deng Pan[a], Kaiyang Chen[a], Qing Zhou[a], Jinjin Zhao[b], Huaijia Xue[a], Yuanjian Zhang[a], Yanfei Shen[a,*]

[a] Medical School, School of Chemistry and Chemical Engineering, Southeast University, Nanjing 210009, China
[b] Department of Clinical Laboratory, The First Affiliated Hospital of Xinxiang Medical University, Xinxiang 453000, Henan, China

ARTICLE INFO

Keywords:
$CdTe@SiO_2$
$SiO_2@CdTe$
Cytotoxicity
Electrochemiluminescent
Immunosensor

ABSTRACT

Electrochemiluminescent (ECL) performance and cytotoxicity of CdTe quantum dots (QDs)-based nanocomposites and its possible application for ECL immunoassay were investigated. Two types of CdTe-based nanocomposites, i.e., SiO_2-coated CdTe ($CdTe@SiO_2$) and CdTe-functionalized SiO_2 ($SiO_2@CdTe$), were synthesized and comprehensively compared in regarding of the cytotoxicity and ECL performance. The in vitro cytotoxicity of $SiO_2@CdTe$ and $CdTe@SiO_2$ nanoparticles was assessed in L02 cells using standard CCK-8 assay, and their ECL performance was investigated by constructing sandwiched immunosensor using $SiO_2@CdTe$ and $CdTe@SiO_2$ as tags for the labelled antibody, respectively. The results showed that $CdTe@SiO_2$ exhibited much lower cytotoxicity and a higher ECL intensity than $SiO_2@CdTe$. Taking the analysis of alpha-fetoprotein (AFP) as an example, the ECL immunosensor using $CdTe@SiO_2$ as an emitter was proved to have a wide linear dynamic range from 1.0 pg mL^{-1} to 100 ng mL^{-1} with a low detection limit of 0.22 pg mL^{-1} (S/N ratio of 3). The ECL immunosensor also demonstrated satisfactory recovery and excellent reproducibility and stability, indicating that this method has prospects in practical application in the clinical diagnosis of AFP.

1. Introduction

Electrochemiluminescence (ECL) has received intense interest in clinical diagnosis (Li et al., 2018), immunoassays (Qin et al., 2018), DNA analysis (Wang et al., 2018), and food and environmental analysis due to its inherent features, such as high sensitivity and simple instrumentation (Farka et al., 2017; Hu and Xu, 2010; Liu et al., 2015; Richter, 2004). Several ECL-active materials, such as luminol, $[Ru(bpy)_3]^{2+}$ and semiconductor crystals, have been chosen as ECL emitters to generate ECL signals (Liu et al., 2018; Zamolo et al., 2012). Among these materials, semiconductor crystals such as CdTe quantum dots (QDs) have been extensively investigated as ECL emitters for the construction of biosensing platforms (Babamiri et al., 2018; Han et al., 2017; Liang et al., 2011), due to their tunable ECL properties, narrow emission bands, good chemical stability, stable ECL emission and easy surface functionalization (Chen et al., 2018b; Hesari et al., 2015; Liu et al., 2016). However, due to the release of the heavy metal Cd^{2+} in aqueous solution, CdTe QDs are highly toxic to biological systems, which has led to restrictions in bioanalytical applications and could further cause health and environmental issues (Derfus et al., 2004; X. Li et al., 2016; Nagy et al., 2012; Su et al., 2010). Thus, it is desirable to develop nontoxic QDs by appropriate surface modification or material design. One effective solution to the problem is to create composite QDs with inert materials (Byrne et al., 2007; Su et al., 2009). Silica (SiO_2) is an optically transparent material that exhibits good water dispersity, biocompatibility and easy surface functionalization. In these regards, SiO_2 is an ideal candidate as a carrier for reducing Cd^{2+} release from CdTe due to its inert nature, high biocompatibility, excellent water solubility and ease of surface functionalization (Hu et al., 2018; Ma et al., 2013).

Moreover, considering the sensitivity of ECL-based biosensing, introducing signal amplification elements for the more sensitive detection of biomarkers is of significant importance (L. Li et al., 2017). Thus, the use of nanomaterials as signal amplifiers is of particular interest for the fabrication of biosensors because of the unique physicochemical properties of nanomaterials (Y. Chen et al., 2017; Y. Li et al., 2016; Wei et al., 2013). SiO_2-based nanomaterials have been widely applied as nanocarriers for signal amplification due to their high surface-to-

* Corresponding author at: Medical School, Southeast University, Nanjing 210009, China.
E-mail address: Yanfei.Shen@seu.edu.cn (Y. Shen).

https://doi.org/10.1016/j.bios.2019.02.022
Received 7 January 2019; Received in revised form 1 February 2019; Accepted 5 February 2019
Available online 19 February 2019
0956-5663/

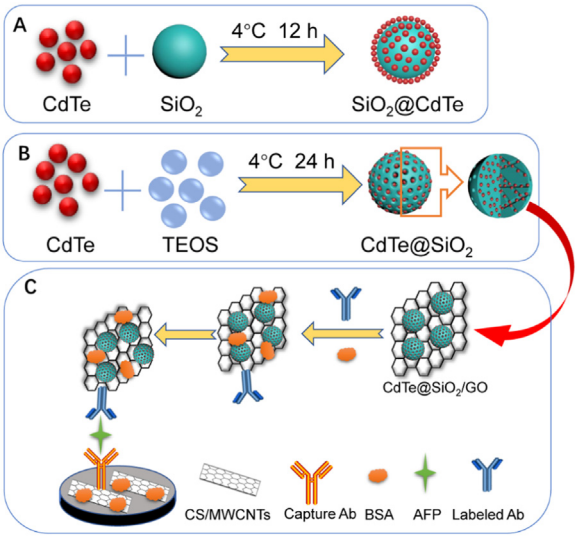

Fig. 1. Scheme (not in scale) of the fabrication and mechanism of the ECL biosensor for AFP detection.

volume ratio and excellent water solubility (Wu et al., 2013; Zhao et al., 2017; Zhou et al., 2016). Thus, it is desirable to use SiO_2 as a nanocarrier of ECL emitters to improve biosensor sensitivity (Chen et al., 2009). Although SiO_2/CdTe nanocomposites have been applied as ECL emitters in pioneer works (Chen et al., 2018a; Dong et al., 2017; Shan et al., 2011), there is no study focusing on both the cytotoxicity and ECL performance of SiO_2/CdTe nanocomposites as yet.

In this study, SiO_2 was selected as both an inert nanomaterial to reduce the toxicity of CdTe QDs and a nanocarrier for signal amplification in ECL immunosensing for the detection of the model tumor biomarker alpha-fetoprotein (AFP) by using CdTe QD-based nanomaterials as ECL emitters. Meanwhile, two types of SiO_2/CdTe nanocomposites, i.e., SiO_2-coated CdTe (CdTe@SiO_2) and CdTe-functionalized SiO_2 (SiO_2@CdTe), were synthesized, and both their cytotoxicity and ECL performance were evaluated. By forming composites with SiO_2 nanoparticles, the cytotoxicity of both nanomaterials substantially decreased, while the ECL efficiency adequately increased. More importantly, CdTe@SiO_2 exhibited much lower cytotoxicity and a higher ECL intensity than SiO_2@CdTe. As a result, CdTe@SiO_2 was employed as an ECL emitter to construct a sandwiched ECL immunosensor (Fig. 1). This work will provide a new avenue for CdTe-based ECL biosensing and extend the application of QDs in clinical fields.

2. Experimental section

2.1. Preparation of CdTe@SiO_2

CdTe@SiO_2 was prepared by a microemulsion (water-in-oil) method (Li et al., 2015; Wang et al., 2014; Zhang et al., 2007). Briefly, 0.18 mL of 1-hexanol was first mixed with 0.177 mL of Triton X-100 and 0.75 mL of cyclohexane in a microcentrifuge tube, followed by adding 0. 1 mL of CdTe (6 mg mL^{-1}) and stirring for 20 min. Then, 0.01 mL of tetraethylorthosilicate (TEOS) and 0.01 mL of (3-aminopropyl)triethoxysilane (APTES) was added to the above solution and stirred for another 20 min. Next, 0.02 mL of $NH_3{\cdot}H_2O$ (25 wt%) was added to the prepared solution and stirred in the dark for another 24 h at 4 °C. Then, the resultant particles were mixed with 1 mL acetone, centrifuged, and washed 3 times with ethanol and water to remove any remaining unreacted CdTe. Finally, the precipitate was redispersed in ultrapure water. The as-obtained amino-functionalized CdTe@SiO_2 nanocomposite was stored in the dark at room temperature.

2.2. Synthesis of SiO_2@CdTe

Briefly, 20 mL of ethanol, 1.21 mL of ultrapure water and 0.9 mL of $NH_3{\cdot}H_2O$ were added to a 50 mL round-bottom flask. After the mixture was heated to 55 °C, 8 mL of ethanol solution containing 0.775 mL TEOS was rapidly added under stirring, and then the mixture continued to react for another 5 h. The resulting SiO_2 nanoparticles were centrifuged, washed and dried in vacuum. After that, 26.95 mg SiO_2 and 0.56 mL APTES were added to 3.34 mL of ethanol, and the mixture was stirred for 5 h. Then, the amino-functionalized SiO_2 nanoparticles were collected by centrifugation. Afterwards, the as-obtained amino-functionalized SiO_2 nanoparticles were added into a solution containing 1-(3-dimethylaminopropyl)-3-ethylcarbodiimide hydrochloride (EDC) and N-hydroxysuccinimide (NHS)-activated CdTe (1 mg mL^{-1}). The mixture was stirred for 12 h at 4 °C. Finally, CdTe-coated SiO_2 nanoparticles (denoted as SiO_2@CdTe) were collected by centrifugation and washed with ethanol and ultrapure water.

2.3. Cell viability assay

The cytotoxicity of the nanoprobes to human hepatocyte (L02) cells was evaluated by the CCK-8 test. Human hepatocyte (L02) cells were seeded in 96-well plates for 24 h at 37 °C under a 5% CO_2 atmosphere, then treated with three different materials, CdTe, SiO_2@CdTe and CdTe@SiO_2, at various concentrations (10, 50, 100 μg mL^{-1}) and incubated for 24 h. A total of 10 μL of CCK-8 solution was added to each well, and cell culture plates were incubated for 1 h. In addition, the viability of L02 cells treated with the same concentration (10 μg mL^{-1}) of nanoprobes for different times was explored. Absorbance values were measured with a microplate reader at 450 nm. The viability of cells was calculated as follows: Viability = ($OD_{test\ group}$-$OD_{blank\ group}$)/($OD_{control\ group}$-$OD_{blank\ group}$) × 100%. All experiments were performed in triplicate.

2.4. Preparation of CdTe@SiO_2-GO labelled AFP antibody (CdTe@SiO_2-GO-Ab_2)

A total of 200 μL graphene oxide (GO) (1 mg mL^{-1}) solution was activated with EDC (20 mg mL^{-1}, 10 μL) and NHS (10 mg mL^{-1}, 10 μL) for 2 h. Then, the activated graphene was collected by centrifugation. After that, 100 μL CdTe@SiO_2 (1.2 mg mL^{-1}) was added to the above precipitate and reacted for 2 h. Then, 20 μL labelled anti-AFP antibody (Ab_2, 100 μg mL^{-1}) was cultured with the nanocomposite for another 12 h at 4 °C in the dark. Next, 100 μL of 1% BSA was added to the solution, and the solution was stirred for 2 h at 37 °C. The resulting CdTe@SiO_2-GO-Ab_2 was obtained by centrifugation and stored under darkness at 4 °C before use.

2.5. Fabrication of ECL immunosensor

As shown in Fig. 1, a sandwich-format ECL immunosensor was fabricated as follows: first, a bare glassy carbon electrode (GCE) was polished into a mirror with 0.3 μm alumina powder, rinsed with water, washed ultrasonically for 5 min in anhydrous ethanol and ultrapure water in turn, and then dried at room temperature. Then, 5 μL of a CS/MWCNT dispersion (1 mg mL^{-1}) was dropped on the GCE and dried at room temperature. Next, 1% glutaraldehyde solution was dropped on the surface of the electrode and incubated at room temperature for 2 h. Afterwards, the CS/MWCNTs/GCE was incubated with the capture anti-AFP antibody (Ab_1) at 4 °C for 12 h. After rinsing with buffer, the resulting Ab_1-modified GCE was blocked by 1% (w/v) BSA in 10 mM PBS (pH 7.4) for 2 h at room temperature. After rinsing, the electrode was then incubated with AFP solution at 37 °C for 40 min. After that, 10 μL of CdTe@SiO_2-GO-Ab_2 solution was cast on the electrode and incubated for 40 min at 37 °C. Finally, the ECL immunosensor for AFP was obtained by rinsing with PBS.

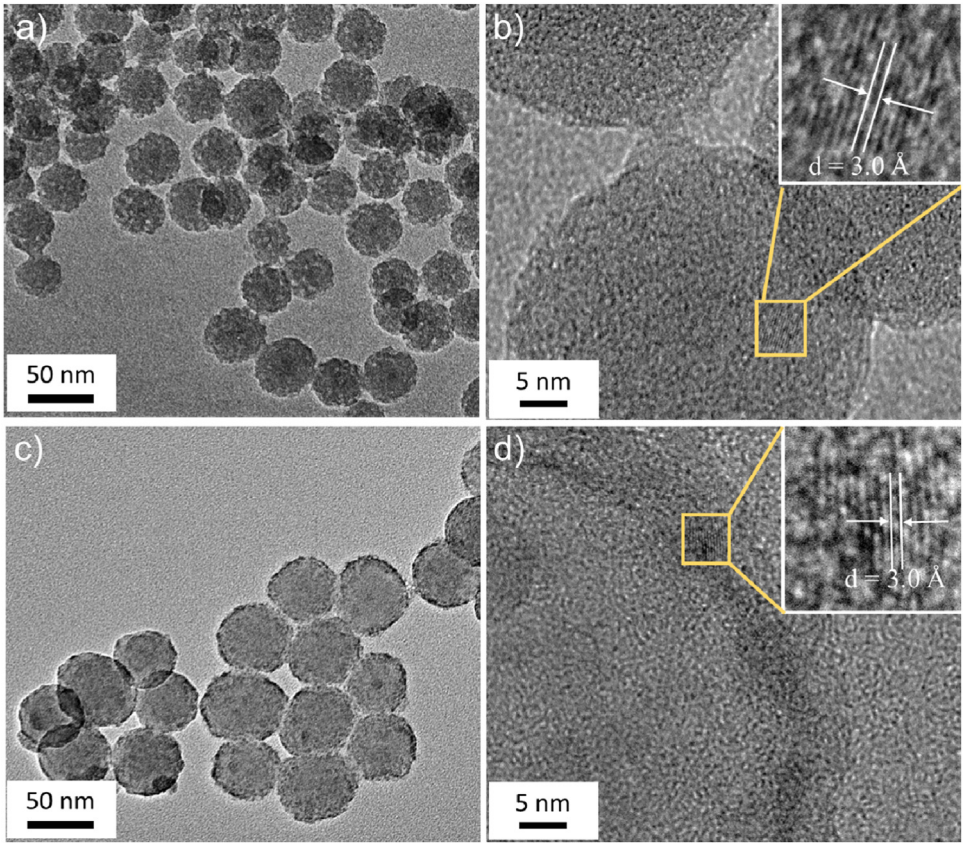

Fig. 2. TEM (a, c) and HRTEM (b, d) images of CdTe@SiO_2 (a, b) and SiO_2@CdTe nanocomposite (c, d). The inset in (b) and (d) is the enlarged HRTEM image, showing CdTe crystalline structure.

3. Results and discussion

3.1. Synthesis and characterization of CdTe@SiO_2 and SiO_2@CdTe

The successful synthesis of CdTe@SiO_2 and SiO_2@CdTe was confirmed by transmission electron microscopy (TEM). As shown in Fig. 2a, the CdTe@SiO_2 exhibited monodispersed meatball-like structures with a diameter of approximately 50 nm and porous structures on the surface. The high-resolution TEM (HRTEM) image showed individual islands in the CdTe@SiO_2 nanocomposites in a crystal lattice with an interplanar spacing of ~3.0 Å (Fig. 2b), which was consistent with the results of HRTEM observation of CdTe QDs (Fig. S1a), indicating that the CdTe nanoparticles were homogenously distributed in the SiO_2 nanospheres. For the synthesis of SiO_2@CdTe nanoparticles, SiO_2 nanoparticles were firstly prepared. As shown in Fig. S1b, SiO_2 nanoparticles exhibited monodispersed spheres with a diameter of ca. 50 nm. After further functionalized with CdTe, the resulted SiO_2@CdTe nanoparticles showed similar spherical structures but with a dark ring on the outer surface of the spherical nanoparticles (Fig. 2c). The HRTEM image of the ring showed a crystal lattice with an interplanar spacing of ~3.0 Å on the ring, confirming the existence of CdTe on the outer surface of these nanospheres (Fig. 2d).

As shown in Fig. 3a, both the SiO_2@CdTe and CdTe@SiO_2 nanohybrids showed similar emission at 590 nm (λ_{ex} = 365 nm), which was also consistent with that of CdTe. The photoluminescence results demonstrated that the physicochemical properties of CdTe were maintained in the nanohybrids (Shan et al., 2011). Further elemental analysis showed that the amounts of CdTe in CdTe@SiO_2 and SiO_2@CdTe were approximately 3.6% and 2.5%, respectively. In addition, the ECL intensities of CdTe, SiO_2@CdTe and CdTe@SiO_2 as different probes for ECL sensing was further investigated, as shown in Fig. 3b, in which Ab_2 was modified with different labels. Compared with the biosensor with CdTe as ECL probe, the ECL intensity of this sensor with SiO_2@CdTe bound to Ab_2 was only enhanced by approximately 12.2%, which could be attributed to the low amount of CdTe (the mass fraction of CdTe in SiO_2@CdTe was 2.5%) and the high resistance of SiO_2 in the SiO_2@CdTe nanohybrid; the observed behavior was consistent with the EIS results of different nanoprobe-modified electrodes (shown in Fig. S2 and Table S1). Interestingly, the ECL intensity of the prepared sensing with CdTe@SiO_2 nanohybrids as probe was enhanced by 80.1% compared to that with CdTe bound to Ab_2, which was much higher than that of SiO_2@CdTe.

To further explore the reason, the surface area of both the CdTe@SiO_2 and SiO_2@CdTe nanoparticles was investigated by Brunauer-Emmett-Teller (BET) analysis of nitrogen adsorption-desorption isotherms. As shown in Fig. 3c and d, the surface area of the CdTe@SiO_2 nanoparticles was approximately 93.911 $m^2\ g^{-1}$, while the surface area of the SiO_2@CdTe nanoparticles was only approximately 45.727 $m^2\ g^{-1}$. The *Barrett-Joyner-Halenda (BJH)* pore size distribution of CdTe@SiO_2 and SiO_2@CdTe obtained from the N_2 adsorption-desorption isotherms (Fig. 3c, d) was shown in Fig. S3. Compared with SiO_2@CdTe, CdTe@SiO_2 showed more evident mesopores ranging from 3 to 10 nm. These results further confirmed the much larger surface area and mesoporous structure of CdTe@SiO_2, which would be responsible for higher CdTe loading. As a result, the high surface area and large amount of CdTe in CdTe@SiO_2 probe would be highly desirable for ECL biosensing.

3.2. Biocompatibility of CdTe, CdTe@SiO_2 and SiO_2@CdTe

The inherent nature of a material, including the shape, size, surface roughness and toxic low-molecular-weight substances remaining from preparation are all related to the biocompatibility of the material. Materials with poor biocompatibility could cause toxicity, irritation,

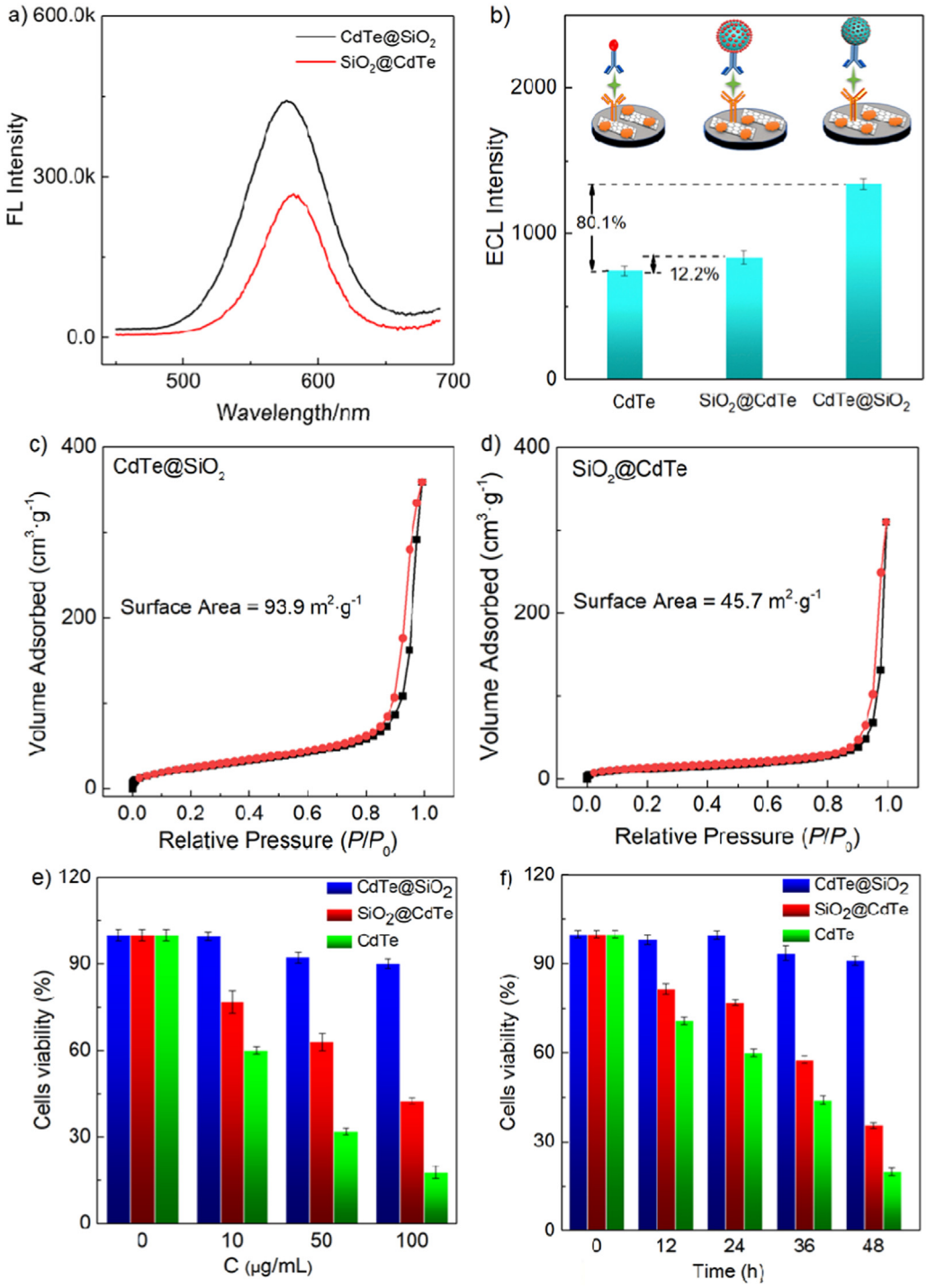

Fig. 3. (a) Photoluminescence spectra for CdTe@SiO_2, and SiO_2@CdTe. (b) The ECL intensities of biosensors with three different nanoprobes labelled on Ab_2, respectively, namely CdTe, SiO_2@CdTe, and CdTe@SiO_2, in 0.1 M PBS (pH 7.4) containing 0.1 M $K_2S_2O_8$ and 0.1 M KCl with 800 V photomultiplier tube (PMT) at a scan rate of 100 mV s^{-1}. BET results of SiO_2@CdTe (c) and CdTe@SiO_2 (d). (e) Cell viabilities of L02 cells treated with different concentrations (0, 10, 50 and 100 μg mL^{-1}) of CdTe, CdTe@SiO_2 and SiO_2@CdTe for 24 h. (f) Cell viabilities of L02 cells treated with CdTe, CdTe@SiO_2 and SiO_2@CdTe (10 μg mL^{-1}) for 0, 12, 24, 36, and 48 h.

teratogenicity and local inflammation in cells and the whole body. Therefore, when considering the use of materials in the biomedical field, biocompatibility is an important indicator that needs to be considered and evaluated. The biocompatibility of three nanoprobes (CdTe, CdTe@SiO_2 and SiO_2@CdTe) was assessed by use of a cell counting kit-8 (CCK-8) assay. As shown in Fig. 3e, a substantial decrease in the viability of L02 cells treated with different concentrations of QDs and SiO_2@CdTe was observed, while CdTe@SiO_2 led to a small reduction in cell activity. For the lowest concentration (10 μg mL^{-1}) of CdTe- and SiO_2@CdTe-treated cells, cell viability fell below 60.0% and 76.8% after 24 h, respectively. In contrast, although the cells were exposed to high concentrations (100 μg mL^{-1}) of CdTe@SiO_2, their activity remained above 90%, indicating that the presence of a SiO_2 outer layer greatly improved the biocompatibility of the QDs (Ou et al., 2014; Su et al., 2009; Yu et al., 2018). In addition, a significant time-dependent decrease in cell viability (in Fig. 3f) was observed. The cell viability decreased to 60.1% and 76.8% after 24 h in CdTe QDs and SiO_2@CdTe, respectively, and decreased to 19.79% and 35.4% after incubation for 48 h, while a small difference (reduction of less than 10%) in L02 cell cytotoxicity was observed within 48 h in the CdTe@SiO_2 group, indicating that CdTe@SiO_2 had lower cell cytotoxicity. Accordingly, the CdTe@SiO2 nanoprobe, which had superior performance, was selected as ECL probes for the immunoassay.

3.3. Fabrication of the electrochemical immunosensor

In this strategy, CS/MWCNTs were dropped on the surface of GCE for Ab_1 loading, and the electron transfer rate increased. Then, a CdTe QD-based signal probe was constructed by coating a CdTe@SiO_2 core-shell structure, which used GO as a substrate for greater Ab_2 immobilization. GO is a novel two-dimensional planar nanomaterial with a special monatomic layer structure; this material has attracted much attention recently because of its excellent electrical conductivity and mechanical properties, such as a high specific surface area and good biocompatibility (Boland et al., 2016; Kong et al., 2017; M. Li et al., 2017; Wang et al., 2015). After forming a sandwich-type structure of Ab_1, AFP, and Ab_2 signal probes, a considerably enhanced ECL signal was obtained in test solution with the CdTe/$S_2O_8^{2-}$-based ECL system.

The fabrication process of the ECL immunosensor was monitored by cyclic voltammetry (CV) measurements. As shown in Fig. S4, the CV of the bare GCE showed a pair of well-defined redox peaks with anodic and cathodic peak potential differences of less than 70 mV, demonstrating a reversible redox reaction process. After the modification of the CS/MWCNTs onto GCE, the peak current increased remarkably, indicating that CS/MWCNTs accelerated the electron transfer on the surface of the electrodes (Gholivand and Mohammadi-Behzad, 2015). The redox peak currents decreased progressively after modification with Ab_1, BSA and AFP due to the electronic hindrance of proteins. All the above results confirmed that the ECL immunosensor was successfully fabricated. To further investigate the possible mechanism of the CdTe-based ECL system in this study, CV and ECL performance of the as-fabricated immunosensor (Fig. S5) were examined. It was found that both the oxygen and $S_2O_8^{2-}$ worked as the co-reactions for the CdTe-based ECL system (see more discussion in ESI).

3.4. Optimization of experimental conditions

The proportion of each component in the CdTe@SiO_2 nanocomposite might be a significant parameter for the ECL response of the CdTe@SiO_2 probe, which will in turn impact the performance of the ECL immunosensor. Thus, the effect of the mass ratio of TEOS (the source material for SiO_2) and CdTe on the ECL response of the immunosensor was examined. As shown in Fig. 4a, as the mass ratio of TEOS and CdTe decreased, the ECL response of the immunosensor increased gradually and reached a maximum when the ratio reached 16:1 in 0.1 M PBS (pH = 7.4) containing 0.1 M KCl and 0.1 M $K_2S_2O_8$, and this response could be ascribed to the enhanced loading of CdTe with an increased SiO_2 amount. When further increasing the mass ratio of TEOS and CdTe, the amount of CdTe in the nanocomposite decreased gradually, reducing the ECL response of the immunosensor. Thus, a ratio of 16:1 for TEOS:CdTe was selected for the following studies. In addition, the effect of the incubation time of Ab_1 and AFP on the ECL intensity of the immunosensor was examined. As shown in Fig. 4b, the ECL response increased gradually with increasing the incubation time and reached a plateau after 40 min, indicating a tendency to complete the immunoreaction on the electrode surface. Thus, 40 min was chosen as the optimized immunoreaction time for Ab_1 and AFP.

3.5. Detection of AFP by the immunosensor

On the basis of the optimized conditions, the sandwiched immunoassay was applied for AFP detection. Fig. 5a displays the ECL profiles for the immunosensor with different concentrations of AFP in 0.1 M PBS containing 0.1 M KCl and 0.1 M $K_2S_2O_8$. The ECL intensities of the sensor increased with increasing AFP concentration. The ECL intensities were linearly related to the AFP concentrations in the range from 1 pg mL^{-1} to 100 ng mL^{-1} with a detection limit of 0.22 pg mL^{-1} (S/N = 3). The linear regression equation could be expressed as $y = 1189.4 \lg c + 3915.6$ with $R^2 = 0.9901$ (Fig. 5b). Furthermore, the proposed ECL immunosensor was compared with other assays for the determination of AFP, as shown in Table 1. The results showed that the sensing performance of the current ECL immunoassay was superior to those of most previous reports. Therefore, except for exhibiting low cytotoxicity, the CdTe@SiO_2 nanohybrid could also be applied as an excellent ECL emitter for immunosensing.

3.6. Stability, reproducibility and specificity of the immunosensor

As a newly developed detection method, the stability, reproducibility and specificity of this ECL sensor are critical for future applications. In Fig. S6, the stability was investigated by continuous cyclic potential scans (n = 11) with a relative standard deviation (RSD) of 3.5%, indicating excellent stability of the ECL signals. Additionally, as shown in Fig. 5c, by storing the immunosensor in 10 mM PBS (pH 7.4) at 4 °C under darkness, 96.9%, 94.8% and 91.3% of the initial signal was retained after storage for 1 d, 3 d and 7 d, respectively. Moreover, the immunosensor still retained 84.6% of the initial signal after 2 weeks, indicating that the proposed immunosensor had satisfactory stability. The reproducibility of the ECL immunosensor for AFP was investigated with intra- and inter-assay precision. The intraassay precision was estimated by assaying one AFP level with five similar measurements with the same immunosensor. The interassay precision was evaluated by measuring one AFP level with five immunosensors. The RSD of the intra- and interassay results obtained for AFP (0.1 ng mL^{-1})

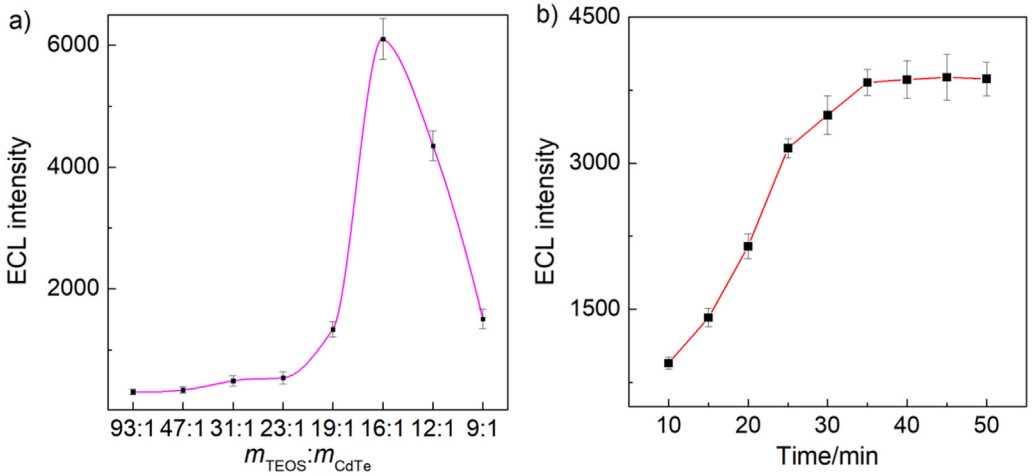

Fig. 4. Optimization of (a) the mass ratio of TEOS and CdTe for the synthesis of CdTe@SiO_2, and (b) the incubation time for AFP (1 ng mL^{-1}) for the detection using the ECL immunosensor. The detection was carried out in 0.1 M PBS (pH 7.4) containing 0.1 M $K_2S_2O_8$ and 0.1 M KCl with 800 V PMT at a scan rate of 100 mV s^{-1}.

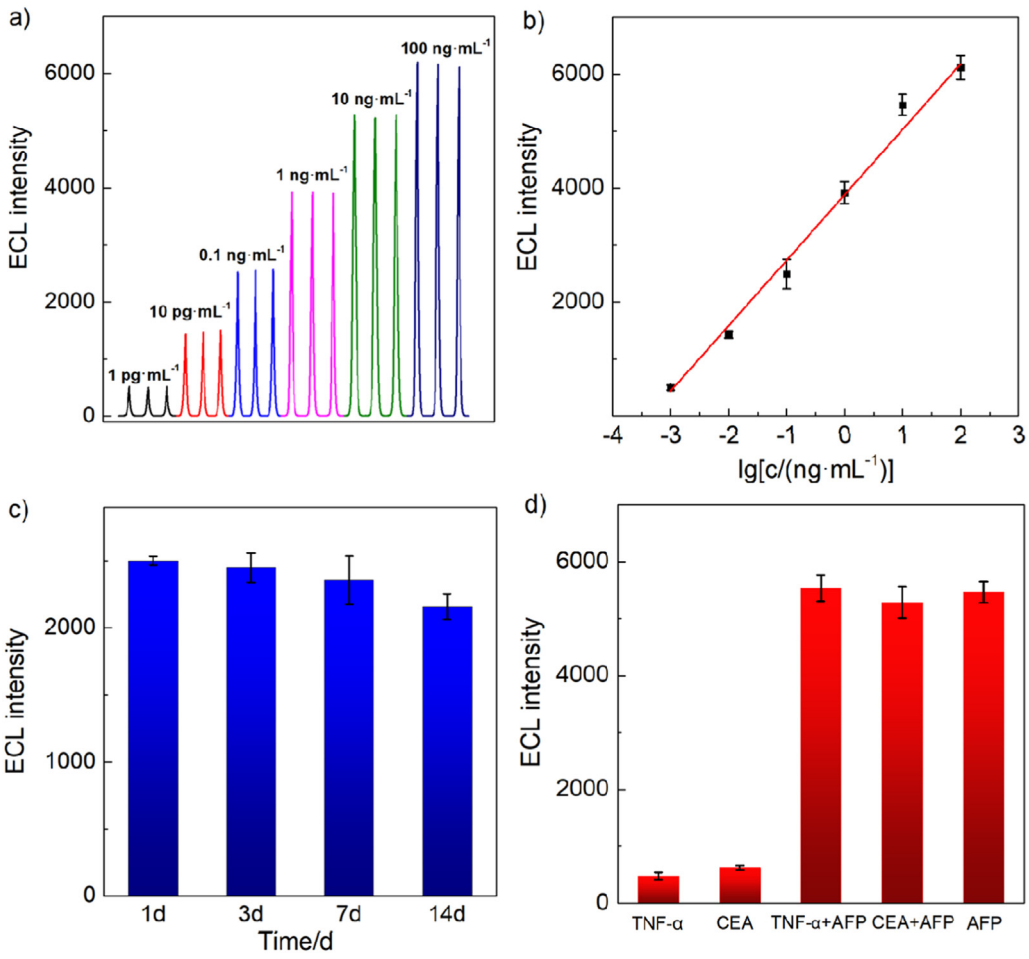

Fig. 5. (a) The ECL intensities of the biosensor for different concentrations of AFP from 1 pg mL^{-1} to 100 ng mL^{-1}. (b) Corresponding calibration curve between the ECL intensity and concentrations of AFP. (c) The stability of the immunosensor after storage for two weeks at an AFP concentration of 0.1 ng mL^{-1}. (d) Selectivity of the proposed immunosensor when employed with TNF-α (10 ng mL^{-1}); CEA (10 ng mL^{-1}); TNF-α (10 ng mL^{-1}) + AFP (10 ng mL^{-1}); CEA (10 ng mL^{-1}) + AFP (10 ng mL^{-1}); and AFP (10 ng mL^{-1}). Error bars: SD, n = 5. The detection was performed in 0.1 M PBS (pH 7.4) containing 0.1 M $K_2S_2O_8$ and 0.1 M KCl with 800 V PMT at a scan rate of 100 mV s^{-1}.

were 4.58% and 4.37%, respectively, indicating that the proposed immunosensor possessed acceptable reproducibility. The specificity of immunosensors plays a significant role in the analysis of real biological samples. Two possible interfering substances, i.e., TNF-α (10 ng mL^{-1}) and CEA (10 ng mL^{-1}), and the mixture of above each substance with AFP were used as interferents to assess specificity. As shown in Fig. 5d, no significant difference was observed in the ECL response for the mixtures compared with that for AFP, while incubation with TNF-α and CEA did not cause an obvious ECL response, suggesting the acceptable specificity of the immunosensor for AFP detection.

3.7. Human serum samples analysis

To investigate the feasibility of the immunosensor for clinical applications, the detection of AFP in human serum was performed with the proposed immunosensor in a recovery experiment. Human serum samples were diluted 40 times with PBS buffer before a standard addition of AFP. The recovery was in the range of 96.5–103.8% (shown in Table S2), indicating that the immunosensor had a good accuracy for the determination of AFP in biological samples.

4. Conclusions

In summary, we investigated the ECL performance of CdTe QDs-based nanocomposites and their possible application for ECL immunoassay were investigated. Two types of CdTe-based nanocomposites, i.e., CdTe@SiO_2 and SiO_2@CdTe, were synthesized. Both their cytotoxicity and ECL performance of CdTe@SiO_2 and SiO_2@CdTe were

Table 1
Comparison of previously reported detection methods for AFP.

No.	Modification method	Linear range (ng mL^{-1})	Detection limit (pg mL^{-1})	Reference
1	Electrochemical immunoassay	0.05–30	5	(Zhao et al., 2013)
2	Electrochemical immunoassay	0.025–15	12	(J. Li et al., 2017)
3	Piezoelectric immunoassay	0.02–4.0	10	(Tang et al., 2010)
4	Fluoroimmunoassay	0.1–750	80	(Hou et al., 2013)
5	Aptamer sensor	0.001–10	0.3	(Zhao et al., 2018)
6	Photoelectrochemical immunoassay	0.05–100	40	(X. Chen et al., 2017)
7	Aptamer-induced fluorescence assay	0.5–60	160	(Xu et al., 2017)
8	Immunosensor	0.05–6	20	(Du et al., 2010)
9	LA-ICPMS	1–500	200	(Hu et al., 2007)
10	Enzyme-linked immunosorbent assay	0.1–11.2	40	(Zhu et al., 2018)
11	Electrochemiluminescence	0.001–100	0.22	This work

LA-ICPMS: Laser ablation inductively coupled plasma mass spectrometry.

assessed. By forming composites with SiO_2 nanoparticles, the cytotoxicity of both nanomaterials substantially decreased, while the ECL efficiency adequately increased. More importantly, CdTe@SiO_2 exhibited much lower cell cytotoxicity due to the inert nature and high biocompatibility of SiO_2 coating on CdTe QDs. Moreover, CdTe@SiO_2 showed 80% enhancement of ECL intensity compared to that of CdTe, while SiO_2@CdTe only exhibited 12.2% ECL enhancement. The much more enhanced ECL performance of CdTe@SiO_2 could be attributed to its large surface area, high CdTe loading, and sufficient bonding sites for biomolecules conjugation. As a result, CdTe@SiO_2 was selected as an ECL emitter for the construction of immunosensor. Taking as the detection of AFP as an example, the as-obtained ECL immunosensor showed superior performance compared to those using other strategies. This work may substantially pave the way for the applications of CdTe-based nanomaterials for bioanalysis in clinical diagnosis.

CRediT authorship contribution statement

Deng Pan: Conceptualization, Methodology, Validation, Formal analysis, Investigation, Data curation, Writing - original draft, Visualization. **Kaiyang Chen:** Methodology, Formal analysis, Visualization. **Qing Zhou:** Methodology, Formal analysis, Investigation. **Jinjin Zhao:** Methodology, Formal analysis, Investigation. **Huaijia Xue:** Methodology, Formal analysis, Investigation. **Yuanjian Zhang:** Methodology, Formal analysis, Investigation, Writing - review & editing, Project administration, Funding acquisition. **Yanfei Shen:** Conceptualization, Methodology, Data curation, Writing - original draft, Writing - review & editing, Visualization, Supervision, Project administration, Funding acquisition.

Acknowledgements

This work is supported by the National Natural Science Foundation of China (21675022 and 21775018), Program from the Natural Science Foundation of Jiangsu Province (BK20170084 and BK20160028) and the Fundamental Research Funds for the Central Universities.

Conflicts of interest

The authors declare no competing financial interest.

Appendix A. Supplementary material

Supplementary data associated with this article can be found in the online version at doi:10.1016/j.bios.2019.02.022.

References

Babamiri, B., Hallaj, R., Salimi, A., 2018. Biosens. Bioelectron. 99, 353–360.
Boland, S., Khan, U., Ryan, G., Barwich, S., Charifou, R., Harvey, A., Backes, C., Li, Z.L., Ferreira, S.M., Möbius, E.M., Young, J.R., Coleman, N.J., 2016. Science 354 (6317), 1257–1260.
Byrne, S.J., Williams, Y., Davies, A., Corr, S.A., Rakovich, A., Gun'ko, Y.K., Rakovich, Y.P., Donegan, J.F., Volkov, Y., 2007. Small 3 (7), 1152–1156.
Chen, L., Chen, C., Li, R., Li, Y., Liu, S., 2009. Chem. Comm. 19, 2670–2672.
Chen, M.M., Wang, Y., Cheng, S.B., Wen, W., Zhang, X., Wang, S., Huang, W.H., 2018a. Anal. Chem. 90 (8), 5075–5081.
Chen, M.M., Wang, Y., Cheng, S.B., Wen, W., Zhang, X., Wang, S., Huang, W.H., 2018b. Anal. Chem. 90 (8), 5075–5081.
Chen, X., Xu, W., Jiang, Y., Pan, G., Zhou, D., Zhu, J., Wang, H., Chen, C., Li, D., Song, H., 2017a. Nanoscale 9 (42), 16357–16364.
Chen, Y., Zhou, S., Li, L., Zhu, J.-J., 2017b. Nano Today 12, 98–115.
Derfus, A.M., Chan, W.C.W., Bhatia, S.N., 2004. Nano Lett. 4 (1), 11–18.
Dong, H., Han, T.-T., Ren, L.-L., Ding, S.-N., 2017. J. Electroanal. Chem. 806, 32–40.
Du, D., Zou, Z., Shin, Y., Wang, J., Wu, H., Engelhard, M., Liu, J., Aksay, I., Lin, Y., 2010. Anal. Chem. 82, 2989–2995.
Farka, Z., Jurik, T., Kovar, D., Trnkova, L., Skladal, P., 2017. Chem. Rev. 117 (15), 9973–10042.
Gholivand, M.B., Mohammadi-Behzad, L., 2015. Mater. Sci. Eng. C 57, 77–87.
Han, T.T., Dong, H., Ren, L.L., Bao, N., Wu, W., Ding, S.N., 2017. Chem. Commun. 53 (39), 5388–5391.
Hesari, M., Swanick, K.N., Lu, J.S., Whyte, R., Wang, S., Ding, Z., 2015. J. Am. Chem. Soc. 137 (35), 11266–11269.
Hou, J., Liu, T., Ren, Z., Chen, M., Lin, G., Wu, Y., 2013. Analyst 138 (13), 3697.
Hu, L., Xu, G., 2010. Chem. Soc. Rev. 39 (8), 3275–3304.
Hu, S., Zhang, S., Hu, Z., Xing, Z., Zhang, X., 2007. Anal. Chem. 79, 923–929.
Hu, Y., Miao, Z.Y., Zhang, X.J., Yang, X.T., Tang, Y.Y., Yu, S., Shan, C.X., Wen, H.M., Zhu, D., 2018. Anal. Chem. 90 (9), 5678–5686.
Kong, X., Liu, Q., Zhang, C., Peng, Z., Chen, Q., 2017. Chem. Soc. Rev. 46 (8), 2127–2157.
Li, D., Qin, Y., Li, H., He, X., Li, W., Zhang, Y., 2015. Biosens. Bioelectron. 66, 224–230.
Li, J., Gao, T., Gu, S., Zhi, J., Yang, J., Li, G., 2017a. Biosens. Bioelectron. 87, 352–357.
Li, L., Chen, Y., Zhu, J.J., 2017b. Anal. Chem. 89 (1), 358–371.
Li, M., Liu, H., Ren, X., 2017c. Biosens. Bioelectron. 89 (Pt 2), 899–905.
Li, X., Lu, P., Wu, B., Wang, Y., Wang, H., Du, B., Pang, X., Wei, Q., 2018. Biosens. Bioelectron. 112, 40–47.
Li, X., Yang, X., Yuwen, L., Yang, W., Weng, L., Teng, Z., Wang, L., 2016a. Biomaterials 96, 24–32.
Li, Y., Sun, L., Liu, Q., Han, E., Hao, N., Zhang, L., Wang, S., Cai, J., Wang, K., 2016b. Talanta 161, 211–218.
Liang, G., Shen, L., Zou, G., Zhang, X., 2011. Chem. (Easton) 17 (37), 10213–10215.
Liu, S., Yuan, H., Bai, H., Zhang, P., Lv, F., Liu, L., Dai, Z., Bao, J., Wang, S., 2018. J. Am. Chem. Soc. 140 (6), 2284–2291.
Liu, S., Zhang, Q., Zhang, L., Gu, L., Zou, G., Bao, J., Dai, Z., 2016. J. Am. Chem. Soc. 138 (4), 1154–1157.
Liu, Z., Qi, W., Xu, G., 2015. Chem. Soc. Rev. 44 (10), 3117–3142.
Ma, Q., Li, Y., Lin, Z.H., Tang, G., Su, X.G., 2013. Nanoscale 5 (20), 9726–9731.
Nagy, A., Steinbruck, A., Gao, J., Doggett, N., Hollingsworth, J., Iyer, R., 2012. ACS Nano 6 (6), 4748–4762.
Ou, J., Wang, F., Huang, Y., Li, D., Jiang, Y., Qin, Q.H., Stachurski, Z.H., Tricoli, A., Zhang, T., 2014. Colloids Surf. B Biointerfaces 117, 466–472.
Qin, X., Gu, C., Wang, M., Dong, Y., Nie, X., Li, M., Zhu, Z., Yang, D., Shao, Y., 2018. Anal. Chem. 90 (4), 2826–2832.
Richter, M., 2004. Chem. Rev. 104, 3003–3036.
Shan, Y., Xu, J.-J., Chen, H.-Y., 2011. Nanoscale 3 (7), 2916.
Su, Y., He, Y., Lu, H., Sai, L., Li, Q., Li, W., Wang, L., Shen, P., Huang, Q., Fan, C., 2009. Biomaterials 30 (1), 19–25.
Su, Y., Hu, M., Fan, C., He, Y., Li, Q., Li, W., Wang, L.H., Shen, P., Huang, Q., 2010. Biomaterials 31 (18), 4829–4834.
Tang, J., Su, B., Tang, D., Chen, G., 2010. Biosens. Bioelectron. 25 (12), 2657–2662.
Wang, C., Qian, J., Wang, K., Wang, K., Liu, Q., Dong, X., Wang, C., Huang, X., 2015. Biosens. Bioelectron. 68, 783–790.
Wang, X., Gao, H., Qi, H., Gao, Q., Zhang, C., 2018. Anal. Chem. 90 (5), 3013–3018.
Wang, Y., Zhao, T., He, X., Li, W., Zhang, Y., 2014. Biosens. Bioelectron. 51, 40–46.
Wei, W., Zhou, J., Li, H., Yin, L., Pu, Y., Liu, S., 2013. Analyst 138 (11), 3253–3258.
Wu, Y., Xue, P., Kang, Y., Hui, K.M., 2013. Anal. Chem. 85 (6), 3166–3173.
Xu, S., Feng, X., Gao, T., Liu, G., Mao, Y., Lin, J., Yu, X., Luo, X., 2017. Anal. Chim. Acta 983, 173–180.
Yu, Z., Hao, R., Zhang, L., Zhu, Y., 2018. Ecotoxicol. Environ. Saf. 156, 75–86.
Zamolo, A.V., Valenti, G., Venturelli, E., Chaloin, O., Marcaccio, M., Boscolo, S., Castagnola, V., Sosa, S., Berti, F., Fontanive, G., Poli, M., Tubaro, A., Bianco, A., Paolucci, F., Prato, M., 2012. ACS Nano 6 (9), 7989–7997.
Zhang, Q., Zhang, L., Liu, B., Lu, X., Li, J., 2007. Biosens. Bioelectron. 23 (5), 695–700.
Zhao, L., Li, S., He, J., Tian, G., Wei, Q., Li, H., 2013. Biosens. Bioelectron. 49, 222–225.
Zhao, M., Li, H., Liu, W., Chu, W., Chen, Y., 2017. Sens. Actuators B 242, 87–94.
Zhao, Y., Yang, Y., Sun, Y., Cui, L., Zheng, F., Zhang, J., Song, Q., Xu, C., 2018. Biosens. Bioelectron. 99, 193–200.
Zhou, J., Liu, Y., Zhang, Z., Yang, S., Tang, J., Liu, W., Tang, W., 2016. Nanoscale 8 (10), 5621–5626.
Zhu, X., Xiong, S., Zhang, J., Zhang, X., Tong, X., Kong, S., 2018. Sens. Actuators B 255, 598–604.